Multiple pattern stability in a photorefractive feedback system

M. Schwab, C. Denz, and M. Saffman

Reprint from the

Annual Report 1998/1999

Licht- und Teilchenoptik

Institut für Angewandte Physik

Technische Universität Darmstadt

Licht- und Teilchenoptik

Institut für Angewandte Physik
Technische Universität Darmstadt
Prof. Dr. Theo Tschudi

Hochschulstrasse 6
D–64289 Darmstadt

Tel.: +49 6151–16 2382
Fax: +49 6151–16 4123

http://www.physik.tu-darmstadt.de
http://gaston.iap.physik.tu-darmstadt.de

Annual Report 1998 / 99

Edited by Markus Kreuzer and Thomas Ganz

ISSN 0930–7168

Multiple pattern stability in a photorefractive feedback system

M. Schwab, C. Denz, and M. Saffman[1]

We report on the observation of a multiple pattern stability regime in a photorefractive single feedback system. While hexagonal patterns are predominant for feedback with positive diffraction length we show that a variety of stable non-hexagonal patterns (square, rectangular or squeezed hexagonal patterns) are generated for certain negative diffraction lengths. We review the linear stability analysis for this system and show that the special shape of the threshold curves in the investigated parameter range gives a first explanation for the occurence of a multiple pattern region [1].

The spontaneous formation of periodic spatial patterns is well-known for a variety of nonlinear optical materials, e. g. atomic vapours, liquid crystals (Kerr slices), organic films or photorefractives [2], where squares and squeezed hexagons were first observed in experiment [3]. Photorefractive materials are well-suited for pattern observation since their intrinsically slow dynamics offers the opportunity to perform real-time measurements and observations. Moreover, low cw laser power in the range of milliwatts is required. In the case of a diffusion-dominated crystal such as $KNbO_3$, no external voltage has to be supplied providing an all-optical pattern formation system. In all these systems, a single-feedback configuration creating two counterpropagating beams in the nonlinear optical medium gives rise to transverse modulational instabilities above a certain threshold of the photorefractive coupling strength. These instabilities generally lead to the formation of hexagonal patterns, which were first reported for a photorefractive system by Honda [2]. Following this pioneering work, various other publications offered improved insight into the stages of pattern formation in these photorefractive materials [4, 5]. A first approach to a nonlinear stability analysis [6] and studies of pattern dynamics due to angular misalignment and competition behaviour were published recently [7, 8, 9]. Our focus of interest is to investigate more complex patterns that may arise in the same configuration for a certain range of the diffraction length without changing the basic interaction geometry. Although some of these patterns were observed previously [3], the appropriate region of instability has not yet been investigated. The basic interaction geometry is depicted in fig. 1. A plane wave of complex amplitude F is incident on a thick photorefractive medium with length l. The backward beam B is produced by reflection at a mirror at a certain position L behind the medium. Our analysis is not restricted

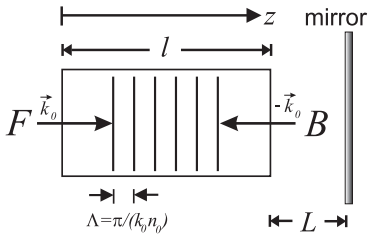

Fig. 1: Basic interaction geometry

to positive diffraction lengths since the $4f-4f$ configuration enables us experimentally to produce negative diffraction lengths which are essential for observing multiple pattern stability. The principle effect of the diffraction length L is to introduce a phase lag of the generated transverse satellite beams relative to the central beam. Throughout the article, we use the normalized diffraction length $n_0 L/l$ as a dimensionless parameter. In this notation, the virtual mirror is inside the crystal for values $-1 \leq n_0 L/l \leq 0$. A diffusion-dominated medium such as $KNbO_3$ offers beam coupling properties which are essential for pattern formation in this configuration. In this case, a dynamic photorefractive grating with a grating vector of $2k_0 n_0$ is written, with k_0 representing the wave number of the incident wave and n_0 the linear refractive index of the crystal. The linear stability analysis presented here is based on the treatment by Honda and Banerjee given in [5]. It is derived from the standard photorefractive two-wave mixing equations (Kukhtarev's equations [10]) and based on the assumption that reflection gratings are dominant in this configuration. For contradirectional two-beam coupling in a diffusion-dominated medium, these equations read as [5]

$$\begin{aligned} \frac{\partial F}{\partial z} - \frac{i}{2k_0 n_0}\nabla_\perp^2 F &= i\gamma \frac{|B|^2}{|F|^2+|B|^2} F \\ \frac{\partial B}{\partial z} + \frac{i}{2k_0 n_0}\nabla_\perp^2 B &= -i\gamma^* \frac{|F|^2}{|F|^2+|B|^2} B \end{aligned} \quad (1)$$

[1]Optics and Fluid Dynamics Department, Risø National Laboratory, Postbox 49, DK-4000 Roskilde, Denmark

z is the direction of propagation, $\nabla_\perp = \frac{\partial^2}{\partial x^2} + \frac{\partial^2}{\partial y^2}$ denotes the transverse Laplacian, and $\gamma = \pi n_1/\lambda \exp(-i\phi)$ is the complex photorefractive coupling constant, representing a measure for amplitude and phase transfer in the photorefractive two-wave mixing process [10]. Here, λ is the wavelength of the incident waves, n_1 is a dimensionless factor measuring the modulation depth of the refractive index grating and ϕ represents the relative phase shift of the refractive index grating with respect to the interference grating written by the beams. For the $KNbO_3$:Fe crystal we used in our experiments, this shift is known to be $\phi = \pi/2$ [11] yielding a purely imaginary coupling constant γ in the notation we use here. This in turn is known to cause pure energy-coupling between the two beams, i. e. energy is transferred from one beam to the other [11]. Performing a linear stability analysis for the system of partial differential equations 1 by applying weak spatial disturbations in the transverse plane and including the boundary conditions (representing the phase lag by feedback) results in a threshold condition for modulational instability (see [5] for details). This reads in a more simplified form as $f(\theta, \gamma, L) = 0$, (θ defines the sideband far field angle in experiment), representing a purely real threshold condition for all parameter values. Given a certain mirror position L, a threshold curve $f(\theta, \gamma) = 0$ can be derived, where the absolute minimum provides information about the unstable sideband angle θ at a certain mirror position (see fig. 2). Figures 3 a) and b) extend previous

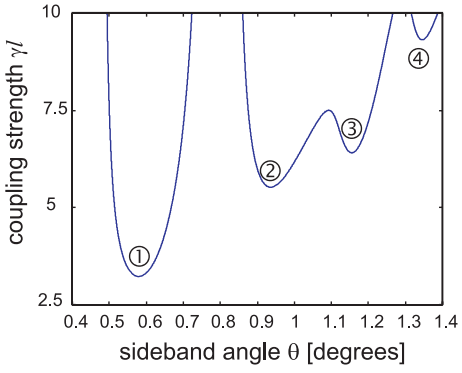

Fig. 2: Example of a threshold curve for $n_0 L/l$=0.6

results of the linear stability analysis [5, 6], taking into account negative diffraction lengths and higher order instability balloons. If the relative minima of the threshold curve (fig. 2) are numbered consecutively, the values of the threshold coupling strength depending on the mirror position for the first to fourth instability "balloon" can be plotted leading

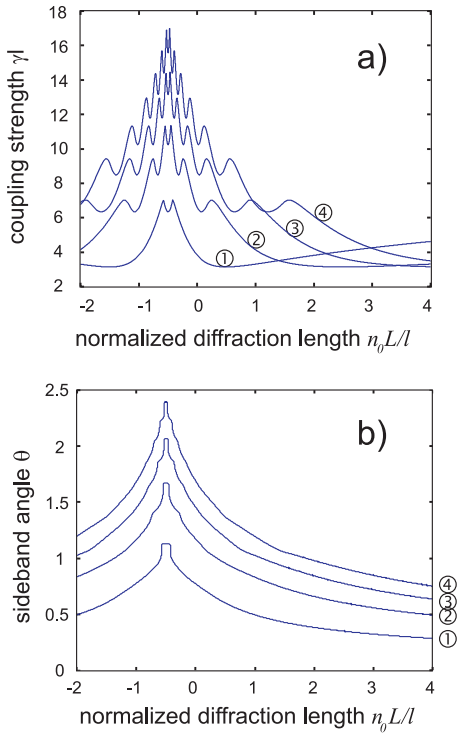

Fig. 3: Results from the linear stability analysis. a) minimal coupling strength for different normalized mirror positions $n_0 L/l$ and b) corresponding sideband angle.

to fig. 3a). The characteristic shape of the curve indicates that the treshold coupling strength has a maximum around $n_0 L/l = -0.5$ which corresponds to a situation where the virtual mirror is situated in the middle of the crystal. This corresponds to previously reported results that for a lower coupling strength, no pattern formation can be observed in this parameter region [7, 8]. Note also the characteristic dip at a value for the diffraction length of $n_0 L/l = -0.5$ and the oscillations appearing for the higher order curves. The corresponding values for the sideband angle θ in the threshold condition lead to the curve displayed in fig. 3b). One can clearly see the abnormal behaviour of the sideband angle-curve (fig. 3b) in a region near $n_0 L/l = -0.5$, where a nearly vertical slope of the curve appears. This typical shape of the curve also appears in the higher order curves and is therefore a special property of this nonlinear feedback system. It may also be a generic feature of negative diffraction lengths in cubic material, but this investigation is not the scope of this paper. However, the special shape of the curves in fig. 3a) and b) may give rise to unexpected patterns in this parameter region. A nonlinear stability analysis is still required for explaining the occurence of different pattern types. The reason for the occurence of these patterns can only be

found by a nonlinear analysis, since a linear stability analysis only accounts for the occurence of a special transverse wavevector to become unstable when excited beyond the instability threshold. We will concentrate on experimental investigations in this parameter region of small negative diffraction lengths. The experimental setup is depicted in fig. 4. Light obtained from a frequency-doubled

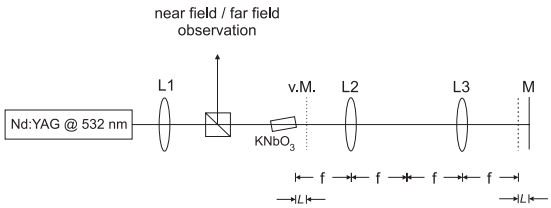

Fig. 4: Experimental setup. M=mirror, v.m.=virtual mirror, L=diffraction length

cw Nd:YAG laser operating at $\lambda = 532$ nm with a coherence length of some meters is focused by lens L1 of focal length f=600 mm onto the exit face of an Iron-doped $KNbO_3$ crystal (l=5 mm), producing a spot with a Gaussian diameter of 320 μm. The crystal was slightly inclined (about 4 degrees) in order to avoid undesired back-reflections from the crystal surfaces. By means of a 4f-2L-4f-system with f=100 mm, the incoming beam is back reflected, thus providing the counterpropagating beam. Considering ABCD-matrix formalism, this configuration can be shown to be completely equivalent to a simple single mirror feedback configuration. Thus, a virtual mirror with a distance of L from the photorefractive medium is obtained. The basic advantage of this system is that negative diffraction lengths can be achieved, which allow to access a broader range of stationary patterns, including squares and rectangles. The laser beam is linearly polarized along the crystal a-axis to exploit the large r_{13} component of the electrooptic tensor in this direction, resulting in a minimum input power for pattern observation of just 0.5 mW. A beam splitter between the focusing lens and the photorefractive medium enables to observe the far field, and by means of a lens and a microscope system, the near field, respectively. The direction of the crystal c-axis is arranged to give rise to depletion of the incoming and amplification of the backward reflected beam, a configuration that is necessary for the observation of transverse structures in this material. The reflectivity of the feedback system including all elements was measured to be $R = 83\%$. For positive diffraction lengths, stable hexagonal patterns are always seen, as depicted in fig. 5a). Higher order harmonics of the hexagonal pattern are clearly apparent in experiment. They saturate the explosive instability of the first order hexagon and are essential for the stability of a hexagonal pattern [6]. This hexagonal structure is well-known to be dominant for many different nonlinear optical materials and is reported for a number of other non-optical pattern forming systems. However, when the virtual mirror is shifted into the crystal, i. e. when negative diffraction lengths are achieved, a remarkable pattern transition occurs: In a small parameter region of the diffraction length around $n_0 L/l = -0.5$, different non-hexagonal structures may appear. Square patterns, squeezed hexagonal, rectangular or parallelogram-shaped structures (see fig. 5 b-e) can be realized as stable pure solutions. The patterns were sta-

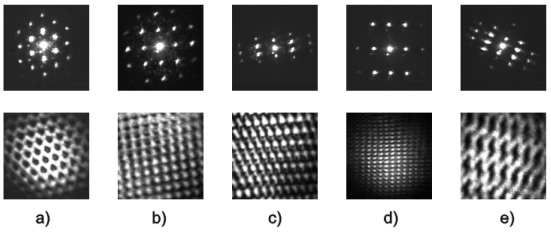

Fig. 5: Experimentally obtained pure pattern states: a) predominant hexagonal structure, b-e) other pattern geometries for the multiple pattern region $n_0 L/l \approx -0.5$. The intensity incident on the crystal was $I = 2.4$ W/cm^2.

ble for a long period of time ($t \gg 1000\tau$), where τ denotes the time constant for this system, in this case defined as the mean build-up time of a pattern which was in the range of $0.5 - 1s$ in the experiments reported here, depending on the input intensity. Temporal alternation of different patterns due to disturbances in the system was also possible on much larger timescales ($t \geq 20s$) than the usual build-up time of a pattern. Besides these pure stable states, also mixed states can be observed, where different patterns coexist with the same or different transverse wave numbers. For this reason, we call this parameter region *multiple pattern region* since a clear parameter-dependent behaviour of the different pattern types was not obtained. A rich variety of patterns was accessible, as well as a large set of transverse $\vec{k}$-vectors as shown in figs. 5, even for the same diffraction length. Outside this multiple pattern region, no other patterns than hexagonal ones can be observed experimentally. Previously [7, 8], we reported a remarkable pattern collapse for the region of negative diffraction length where we now observe multiple patterns. The pattern collapse, or absence of patterns, was explained as a result of the photorefrac-

tive coupling strength being too low for the observation of transverse structures. In the experiments reported here a different crystal was used with about twice as large nonlinearity ($\gamma l \approx 4$) which accentuates the necessity of sufficient nonlinearity for observing non-hexagonal patterns in the regime of negative diffraction length. Though a nonlinear stability analysis has not been performed for negative diffraction lengths, detailed investigations of the results of the linear stability analysis taking into account higher order instability balloons may already give useful information about the pattern type. Figure 6 shows the measured values for the hexagon instability angle θ in the far field as a function of the normalized diffraction length n_0L/l together with the theoretical results of the linear stability analysis (first and second instability balloon). The measured values agree well with the

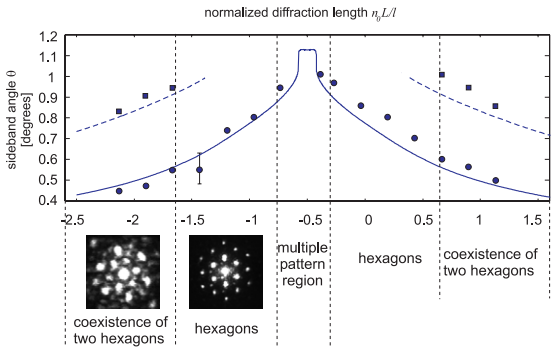

Fig. 6: Sideband angle θ as function of the normalized diffraction length n_0L/l for an incident intensity of $I = 2.4$ W/cm^2. The theoretical curve is displayed together with experimental values for the transverse scale (circles and squares).

theoretical curves. As predicted in [7], a coexistence of two transverse $\vec{k}$-vectors appears for larger positive or negative diffraction length as indicated in the figure. Here, a second instability balloon (see fig. 3 in [7]) takes the absolute minimum of the instability curve thus leading to a degeneration of the transverse wave-vector. This leads to a coexistence of two hexagons on two transverse scales tilted by 30 degrees relative to each other. The multiple pattern region described earlier is also indicated in the figure. A large number of various transverse $\vec{k}$-vectors occur for $-0.7 \leq n_0L/l \leq -0.3$, being too numerous to be displayed in fig. 6. One can clearly see that for parameter values $n_0L/l = -0.57$ and $n_0L/l = -0.43$ the curve in fig. 6 shows a nearly vertical slope indicating that a whole band of transverse $\vec{k}$-vectors will participate in the stage of pattern formation, thus explaining the possibility for a variety of transverse $\vec{k}$-vectors. Nevertheless, the observed sideband angles in the multiple pattern region do not necessarily lie on the curve. Moreover, this explanation does not hold for $n_0L/l = -0.5$ (flat region of this curve) where sideband angles up to 2.7 degrees could be observed for the case of rectangular patterns. This problem is still under investigation.

In conclusion, we have analyzed a parameter region where a photorefractive feedback system produces a variety of different spatial patterns. With our experimental configuration, we are able to access a broader parameter region including negative diffraction lengths, which allow the observation of squares, squeezed hexagonal or rectangular patterns. The occurence of nonhexagonal patterns is restricted to a small parameter region where the virtual mirror is placed inside the crystal. This *multiple pattern region* coincides with an unusual shape of the corresponding curves for pattern size vs. diffraction length derived from a linear stability analysis. This is, to the best of our knowledge, the first observation of a multiple pattern parameter region. This observation may not be restricted to photorefractives and could be observed in other optical pattern forming systems.

References

[1] M. Schwab, C. Denz, M. Saffman, Appl. Phys. B **69**, 429 (1999).

[2] T. Honda, Opt. Lett. **18**, 598 (1993).

[3] T. Honda, H. Matsumoto, M. Sedlatschek, C. Denz, T. Tschudi, Opt. Comm. **133**, 293 (1997).

[4] M. Saffman, A.A. Zozulya, D.Z. Anderson, J.Opt.Soc.Am.B **11**, 1409 (1994).

[5] T. Honda, P.P. Banerjee, Opt. Lett. **21**, 779 (1996).

[6] P.M. Lushnikov, JETP **86**, 614 (1998).

[7] C. Denz, M. Schwab, M. Sedlatschek, T. Tschudi, T. Honda, J.Opt.Soc.Am.B **15**, 2057 (1998).

[8] M. Schwab, M. Sedlatschek, B. Thüring, C. Denz, T. Tschudi, Chaos, Solitons Fractals Vol. **10**, 701 (1999).

[9] A.V. Mamaev, M. Saffman, Opt. Lett. **22**, 283 (1997).

[10] N.V. Kukhtarev, V.B. Markov, S.G. Odulov, M.S. Soskin, V.L. Vinetskii, Ferroelectrics **22**, 961 (1979).

[11] L. Solymar, D.J. Webb, A. Grunnet-Jepsen, *The Physics and Applications of Photorefractive Materials*, Clarendon Press, Oxford (1996).

